Falloff curve and specific rate constants for the reaction nitrogen dioxide + nitrogen dioxide .dblarw. nitrogen oxide (N2O4)

ARTICLE *in* THE JOURNAL OF PHYSICAL CHEMISTRY · JULY 1988

Impact Factor: 2.78 · DOI: 10.1021/j100326a027

3 AUTHORS, INCLUDING:

Carlos J. Cobos
National Scientific and Technical Research C…
126 PUBLICATIONS **3,032** CITATIONS
SEE PROFILE

Klaus Luther
Georg-August-Universität Göttingen
117 PUBLICATIONS **1,975** CITATIONS
SEE PROFILE

diones further supports this mechanistic hypothesis. Listed in Table III are the ketones and diones for which we have recently determined the temperature dependence of OH reactivity along with an indication of the type of CH_3 and/or CH_2 groups responsible for reactivity. Clearly, for both acetone and 2,3-butanedione, where only α components react, a positive activation energy of approximately 1 kcal/mol is observed. For 2-butanone and 3-pentanone, where β reactivity (proceeding through formation of an adduct intermediate) accounts for almost 30% of the reaction rate (at room temperature), the activation energies drop to values much closer to zero. Finally, for 2,5-hexanedione, where the majority of the molecule's reactivity involves the β-CH_2 groups, a strong "negative activation energy" is calculated.

Still further support for this hypothesis comes from our present kinetic data for the reaction of OH with the cyclic ketones. The formation of such a six-membered ring (adduct) is, of course, not possible for these cyclic ketones and, indeed, we do not find any evidence for an enhanced reactivity of the β position. Thus, the room temperature reactivity per $-CH_2-$ group is the same (within experimental error) in cyclobutanone as in cyclobutane, in cyclopentanone as in cyclopentane, and in cyclohexanone as in cyclohexane using the rate constant values recommended by Atkinson[11] for the cyclic alkanes.

Finally, we should note that our room temperature gas-phase rate constant for the 2,3-butanedione reaction is very similar to the corresponding solution phase rate constant (2.82×10^{-13} cm^3 molecule^{-1} s^{-1}).[12] Such agreement between OH rate constants measured in the two different phases has been tabulated for many organic oxygenates where adduct formation does not play an important role.[13] For 2,4-pentanedione, the solution phase rate constant (1.64×10^{11} cm^3 molecule^{-1} s^{-1})[12] is one order of magnitude higher than the gas-phase rate constant measured in the present work. This difference is inconsistent with our comparative analysis for reactions proceeding via simple H-atom abstraction. Since the measured gas-phase rate constant agrees with the value predicted from the sum of $2[\alpha\text{-}CH_3] + [\alpha\text{-}CH_2]$ group reactivities, we suggest that the solution-phase study has overestimated the rate constant for this dione.

Acknowledgment. The research described herein was conducted with the partial support of the National Aeronautics and Space Administration (Agreement W-15, 816).

Registry No. OH*, 3352-57-6; 2,3-butanedione, 431-03-8; 2,4-pentanedione, 123-54-6; 2,5-hexanedione, 110-13-4; cyclobutanone, 1191-95-3; cyclopentanone, 120-92-3; cyclohexanone, 108-94-1.

(11) Atkinson, R. *Chem. Rev.* **1986**, *86*, 69.

(12) Buxton, G. V.; Greenstock, C. L.; Ross, A. B. *J. Phys. Chem. Ref. Data*, in press.

(13) Wallington, T. J.; Dagaut, P.; Kurylo, M. J. *J. Phys. Chem.*, in press.

Falloff Curve and Specific Rate Constants for the Reaction $NO_2 + NO_2 \rightleftharpoons N_2O_4$

Peter Borrell,[†] C. J. Cobos,[‡] and K. Luther*

Institut für Physikalische Chemie der Universität Göttingen, Tammannstrasse 6, D-3400 Göttingen, West Germany *(Received: November 13, 1987)*

The rate of association of NO_2 to N_2O_4 was measured in N_2 at pressures from 1 to 207 bar. This way the reaction was observed in a large section of its falloff range. The relaxation of NO_2/N_2O_4 mixtures was followed after laser flash photolysis of N_2O_4 at 248 nm. From the results the falloff curve was constructed, which gives the high- and low-pressure rate constants at 298 K (in cm^3 molecule^{-1} s^{-1}): $k_{ass}^{\infty} = (8.3 \pm 1.0) \times 10^{-13}$ and $k_{ass}^{0} = (1.4 \pm 0.2) \times 10^{-33}[N_2]$. Earlier measurements, believed to be in the low-pressure regime, have not been free from falloff effects. The low value of k^{∞} was analyzed with the statistic adiabatic channel model, and specific rate constants, $k(E,J)$, were calculated. They increase very steeply with energy just above the reaction threshold and go through maxima at low excess energies. These unusual effects are analyzed theoretically and the strong contributions are pointed out of the low-frequency vibrations which "disappear" during the dissociation of N_2O_4.

Introduction

The NO_2/N_2O_4 association/dissociation

$$NO_2 + NO_2 \rightleftarrows N_2O_4 \qquad (1,-1)$$

was one of the first gas-phase reactions to be considered kinetically. More than a century ago in 1885, Natanson[1] concluded, from measurements of the sound velocity in NO_2/N_2O_4 mixtures, that N_2O_4 could be dissociated in acoustic pressure waves. The determination of the reaction rate from sound dispersion measurements was suggested by Keutel and Nernst[2] in 1910 and put on a theoretical basis by Einstein[3] in 1920. Early experiments were largely unsuccessful[4] because of the limitations of the apparatus available. Later, improvements in sound dispersion and absorption techniques allowed the rate constant to be determined at temperatures between 273 and 320 K in several bath gases below 1 bar pressure.[5,6] In a pioneering study Carrington and Davidson[7] used weak, dispersed shock waves to induce temperature and pressure jumps in NO_2/N_2O_4 mixtures. They observed the relaxation to equilibrium between 250 and 300 K at pressures up to about 7 bar. In addition, the easily accessible and thermodynamically well-characterized NO_2/N_2O_4 system has been used to demonstrate the feasibility of new experimental methods in gas kinetics.[5,8,9] Nevertheless, the measured data are still scattered

[†] Permanent address: Department of Chemistry, Keele University, Staffordshire, Great Britain.

[‡] Permanent address: Instituto de Investigaciones Fisicoquímicas Teóricas y Aplicadas (INIFTA), La Plata, Argentina.

(1) Natanson, E.; Natanson, L. *Wied. Ann. Phys.* **1885**, *24*, 454; **1886**, *26*, 606.

(2) Nernst, W. cited in: Keutel, F. Doctoral Thesis, Berlin, 1910.

(3) Einstein, A. *Sitzungsber. Preuss. Akad. Wiss. Phys.-Math. Kl.* **1920**, *18*, 380.

(4) Argo, W. L. *J. Phys. Chem.* **1914**, *18*, 438. Selle, H. *Z. Phys. Chem.* **1923**, *104*, 1. Grüneisen, E.; Goens, E. *Ann. Phys.* **1923**, *72*, 193. Kistiakowsky, G. B.; Richards, W. T. *J. Am. Chem. Soc.* **1930**, *52*, 4661. Brass, P. D.; Tolman, R. C. *J. Am. Chem. Soc.* **1932**, *54*, 1003.

(5) (a) Richards, W. T.; Reid, J. A. *J. Chem. Phys.* **1933**, *1*, 114. Sessler, G. *Acustica* **1959**, *9*, 119; **1960**, *10*, 44. Blend, H. *J. Acoust. Soc. Am.* **1970**, *47*, 757. (b) Cher, M. *J. Chem. Phys.* **1962**, *37*, 2564.

(6) Zimet, E. *J. Chem. Phys.* **1970**, *53*, 515.

(7) Carrington, T.; Davidson, N. *J. Phys. Chem.* **1953**, *57*, 418.

(8) Bauer, S. H.; Gustavson, M. R. *Discuss. Faraday Soc.* **1954**, *17*, 69. Brokaw, R. S. *J. Chem. Phys.* **1961**, *35*, 1569.

0022-3654/88/2092-4377$01.50/0

and incomplete. Only a few direct observations of the association reaction 1 have been reported[9,10] but, as the equilibrium constant is accurately known, k_{-1} and k_1 can be interconverted without loss of accuracy and so the determination of one constant is entirely equivalent to the determination of the other.

Comparatively little has been published on the pressure dependence of the rate constants in order to determine the extent of the falloff range and to deduce the limiting high-pressure rate constant. Deviations from pure second-order behavior in the dissociation have been observed early on at pressures of a few bar,[7] but the rate constants determined at pressures below 1 bar have generally been interpreted[11,12] as limiting low-pressure rate constants, k^0. The gradual onset of deviations from low-pressure behavior, however, is difficult to measure with sufficient accuracy when the experimental data cover only the initial part of a broad falloff curve.[13] The present work shows that the assumption of simple second-order kinetics leads to values of low-pressure rate constants k^0 which are systematically too small. This point has also been emphasized in recent studies of recombination reactions to form CH_3O_2[14] and N_2O_5[15] where a proper analysis of the results was only possible when extended measurements of the falloff curve were included. An analysis of the NO_2/N_2O_4 association–dissociation kinetics by means of unimolecular rate theory is of special interest. The bond dissociation energy of N_2O_4, 53.2 kJ mol^{-1}, is substantially lower than that of most previously studied molecules. In addition, N_2O_4 has several low-frequency vibrational modes which disappear at the dissociation of the N–N bond. This system is therefore a promising candidate to look for unusual kinetic properties. It turns out that the disappearing low-frequency oscillators of N_2O_4, which become product rotors in NO_2, are responsible for a very low value of the high-pressure rate constant k^∞ and an unusual energy dependence of the specific rate constants $k(E,J)$.

In the following we report measurements of the NO_2 association over a range of pressures from 1 to 200 bar of added nitrogen. A large part of the falloff curve of this reaction can thus be covered. The limiting rate constants k_1^0 and k_1^∞ are evaluated by a thorough falloff analysis.[16] On the basis of this measured k_1^∞ we then have used the simplified statistical adiabatic channel model[17] to calculate the energy and angular momentum resolved specific rate constants, $k(E,J)$. Surprisingly, these calculations showed pronounced maxima of the rate constants at very low energies and on physically accessible time scales, a feature which has not been recognized before. The conditions for the occurrence of this behavior are therefore explored in some detail.

Experimental Section

The reaction was studied in equilibrium mixtures of N_2O_4 and NO_2 together with added nitrogen. N_2O_4 was photolyzed with 20-ns pulses from a KrF excimer laser at 248 nm. The relaxation of the system back to equilibrium was observed by measuring the change in absorption at 220 nm.

A more detailed description of the experimental arrangement has appeared previously[14] and only an outline will be given here. The reaction vessel was a stainless-steel high-pressure cell with a crossed-beam geometry for the photolysis and analysis beams. A homogeneously irradiated reaction zone inside the cell was defined by suitable diaphragms, the absorption path for the analysis beam being 20 mm. The analysis light from a 200-W Hg–Xe high-pressure arc, used in a pulsed mode to increase the UV intensity, passed through the cell to a prism monochromator and was then recorded with a photomultiplier and an oscilloscope. An interference filter and a shutter were inserted between the lamp and the cell in order to minimize the photolysis of NO_2 by analysis light. The shutter was opened for only 40 ms during each experiment. This way no photolysis of NO_2 could be detected, even after several hundred absorption measurements of the same sample. Thus, with a single sample, we could make a whole range of measurements of absorption coefficients and the equilibrium constant at increasing pressure of N_2 bath gas.

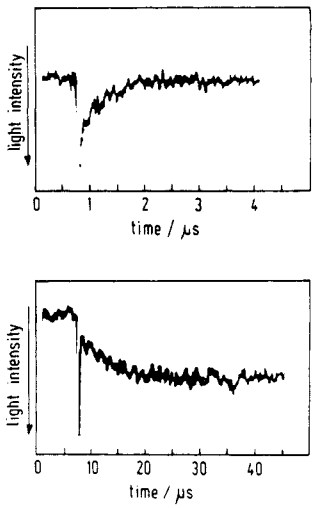

Figure 1. Absorption–time profiles in N_2O_4/NO_2 mixtures at 298 K after laser pulse photolysis at 248 nm. Observation at 220 nm. (a, top) 160 bar of N_2; the system relaxes by NO_2 association back to the initial equilibrium. (b, bottom) 1 bar of N_2; a laser-induced temperature jump ($\simeq$0.8 K) occurs; the initial photodissociation step is followed by further N_2O_4 dissociation toward the new equilibrium.

The temperatures of the experiments were close to 298 K; a check was made on the exact temperature for each shot using the initial absorption and the strongly temperature-dependent equilibrium constant. Low pressures were measured with capacitance manometers, and a Bourdon gauge was used at higher pressures. We purified the N_2O_4/NO_2 from NO by addition of oxygen and distillation. Commercially available high-purity nitrogen (99.996%) was used.

The laser fluence was 100 mJ cm^{-2} at 248.4 nm. At this wavelength the absorption coefficient of N_2O_4 is $\simeq$90 times that of NO_2[18] such that the NO_2 concentration is practically not affected by laser photolysis. In a laser flash where typically 5% of the N_2O_4 were dissociated, only a fraction of $\lesssim 5 \times 10^{-4}$ of the NO_2 was photolyzed. The experiments were made with 5–50 Torr of the N_2O_4/NO_2 mixture, most of them with 20 Torr. For 20 Torr and 298 K, the equilibrium ratio NO_2/N_2O_4 is then 5.84 such that 94% of the molecules that absorb a laser photon are N_2O_4 and only 6% NO_2. Figure 1a shows an experimental trace in which the initial decrease in absorption, due to the dissociation of N_2O_4, is followed by NO_2 recombination back to the equilibrium. This form of a signal was observed at most pressures; but at the lowest pressures studied the character of the trace changed, as Figure 1b illustrates. Here, after the initial photodissociation, further thermal dissociation occurs which corresponds to the relaxation to a new equilibrium state at a somewhat increased temperature. The effect can readily be understood if it is remembered that most of the photon energy ($\simeq$460 kJ mol^{-1}) after photodissociation of N_2O_4 is still available to heat the gas. Molecular beam experiments[19] have shown that, on photolysis at 248 nm, the NO_2 fragments are electronically excited and that

(9) Wegener, P. P. *J. Chem. Phys.* **1958**, *28*, 724; *Phys. Fluids* **1959**, *2*, 264; *J. Chem. Phys.* **1964**, *41*, 1512.
(10) Gozel, P.; Calpini, B.; van de Bergh, H. *Isr. J. Chem.* **1984**, *24*, 210.
(11) Baulch, D. L.; Drysdale, D. D.; Horne, D. G. *Evaluated Kinetic Data for High Temperature Reactions*; Butterworths: London, 1973; Vol. 2.
(12) Schofield, K. *J. Phys. Chem. Ref. Data* **1973**, *2*, 25.
(13) Recent measurements at higher pressures in He and Ar, leading further into the falloff range, are reported by Gozel, P. Thesis, Lausanne, 1985. The results are in good agreement with the present work.
(14) Cobos, C. J.; Hippler, H.; Luther, K.; Ravishankara, A. R.; Troe, J. *J. Phys. Chem.* **1985**, *89*, 4332.
(15) Croce de Cobos, A. E.; Hippler, H.; Troe, J. *J. Phys. Chem.* **1984**, *88*, 5083. Malko, M. W.; Troe, J. *Int. J. Chem. Kinet.* **1982**, *14*, 399.
(16) The experimental results of this work have been presented at the 8th International Symposium on Gas Kinetics, Nottingham, GB, 15–20 July 1984.
(17) Troe, J. *J. Chem. Phys.* **1983**, *76*, 6017.
(18) Hall, T. C.; Blacet, F. E. *J. Chem. Phys.* **1952**, *20*, 1475. Bass, A. M.; Ledford, A. E.; Laufer, A. H. *J. Res. Natl. Bur. Stand.* **1976**, *80A*, 143.
(19) Kawasaki, M.; Kasatani, K.; Sato, H.; Shinohara, H.; Nishi, N. *Chem. Phys.* **1983**, *78*, 63.

the translational energy distribution peaks near 50 kJ mol^{-1}. Collisional energy transfer from the hot photoproducts will lead to a heating in the reaction zone and a sizeable temperature jump at sufficiently low pressures. At 1 bar total pressure the change between the initial and the final absorption indicated a temperature jump of 0.8 K. Clearly at some pressure a little above 1 bar the final NO_2 product concentration should just equal that formed in the photodissociation: such records were obtained, where the initial change due to photodissociation is followed by a constant absorption level throughout the time of observation. At pressures below about 1 bar the UV excitation of N_2O_4/NO_2 at 248 nm acts as a genuine temperature jump technique. It has the advantage that no sensitizer needs to be added in the system. The alternative method of using a CO_2 laser to induce a temperature jump requires an additional absorber like SF_6 or SiF_4 to act as an energy-transfer reagent,[10] which may lead to complications.

Standard kinetic analysis shows that, for perturbations close to the equilibrium, the association of NO_2 can be described by a first-order kinetic equation

$$k_r = \frac{1}{\Delta[N_2O_4]} \frac{d\Delta[N_2O_4]}{dt} \quad (2)$$

where $\Delta[N_2O_4]$ is the difference between the actual N_2O_4 concentration at a time t and its final value $[N_2O_4]_f$: $\Delta[N_2O_4] = [N_2O_4] - [N_2O_4]_f$. This linear approximation neglects the quadratic term $-4k_1(\Delta[N_2O_4])^2$. k_1 is then evaluated from

$$k_1 = k_r/(4[NO_2]_f + K_{c,f}) \quad (3)$$

At high bath gas pressures, the system relaxes practically back to the initial conditions so that initial and final concentrations and equilibrium constants are the same, $[NO_2]_f = [NO_2]_i$ and $K_{c,f} = K_{c,i}$. But at low pressure, where a temperature jump is induced the observed relaxation leads to a final state with $K_{c,f} > K_{c,i}$ and $[NO_2]_f > [NO_2]_i$. The calculation of $K_{c,f}$ and $[NO_2]_f$ from the absorbance, $A_{220,f}$, at the end of the observed relaxation is straightforward. The change in K_c at 1 bar pressure is approximately 25%, and this decreases to ~6% at 10 bar of N_2 pressure. Even at our lowest pressures, the temperature changes occur in a time short in comparison to the chemical relaxation, and so the rate constants are evaluated at the final temperatures.

Results

Pressure Dependence of the Equilibrium Constant and the Absorption Coefficients. To evaluate the rate constants correctly from the measurements at high pressures it is necessary to know how the absorption coefficients and the equilibrium constant change with the pressure of added bath gas. For this purpose series of optical transmission measurements were made at 436 and 404 nm, where only NO_2 absorbs, and at 220 nm, where the N_2O_4 absorption dominates. The transmission of the cell itself, containing only nitrogen, was checked and found to increase by 2% on increasing the pressure from 1 to 200 bar in good agreement with values calculated from Fresnel's equation with the pressure-dependent refractive index of N_2.

High-pressure absorption measurements were made with various samples of N_2O_4/NO_2 mixtures at pressures between 5 and 20 mbar. In each case the manometrically determined concentration was checked initially by optical absorption data and good consistency was obtained by using the known values of K_c.[20] Then to each sample N_2 bath gas was added, and the pressure was raised in steps from 1 to 200 bar; the transmission was recorded at each intermediate pressure after leaving sufficient time for a complete mixing.

Both K_c and ϵ can be found from the absorption of a series of mixtures at a particular bath gas pressure. If, for a sample of N_2O_4/NO_2 a concentration, S_N, is defined in terms of the total content of NO_2 present either as NO_2 itself or as N_2O_4

$$S_N = 2[N_2O_4] + [NO_2]$$

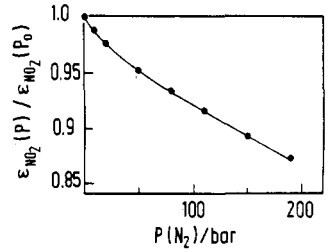

Figure 2. Relative pressure dependence of the absorption coefficient of NO_2 at 426 nm; 1 to 200 bar of N_2 ($\epsilon_{NO_2}(p_0 = 1\ bar) = 155\ dm^3\ mol^{-1}\ cm^{-1}$; for spectral parameters see text).

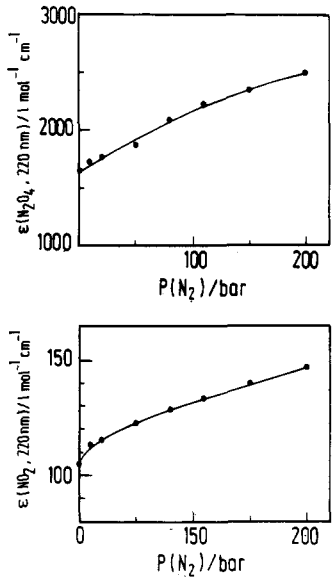

Figure 3. Absorption coefficients of N_2O_4 (a, top) and NO_2 (b, bottom) at 220 nm as a function of the N_2 bath gas pressure.

then S_N can be expressed in terms of the absorbance at 436 nm, A_{436} (=log $(I_0/I)_{436}$)

$$S_N = \frac{2A_{436}^2}{(\epsilon_{436}^{NO_2} l)^2 K_c} + \frac{A_{436}}{\epsilon_{436}^{NN_2} l} \quad (4)$$

where l is the path length of the absorption cell. Thus if S_N/A_{436} is plotted against A_{436} for varying N_2O_4/NO_2 samples at the same bath gas pressure, K_c and $\epsilon_{436}^{NO_2}$ can be determined from slope and intercept of the resulting straight lines. The observed pressure dependence of the absorption coefficient of NO_2 at 436 nm, $\epsilon_{436}^{NO_2}$, is shown in Figure 2. It can be seen that the absorption coefficients decline by ≃13% over the pressure range studied. The low-pressure value $\epsilon(P_0)$ in the banded part of the NO_2 spectrum was found to be 155 $dm^3\ mol^{-1}\ cm^{-1}$ for the 435.7-nm Hg line from our lamp (3.1 nm fwhh) and a matched 3.2-nm bandwidth of the monochromator in good agreement with earlier work.[18,21] The absorption at 404.7 nm was also measured and treated in the same way. A similar decrease in ϵ with increasing pressure was found. At 220 nm, where both N_2O_4 and NO_2 absorb, $\epsilon_{220}^{NO_2}$ and $\epsilon_{220}^{NO_2}$ were found from the absorbance, A_{220} (=log $(I_0/I)_{220}$), by comparing A_{220} with A_{436}. Then

$$\frac{A_{220}}{A_{436}} = \epsilon_{220}^{NO_2} A_{436} K_c l/(\epsilon_{436}^{NO_2})^2 + \frac{\epsilon_{220}^{NO_2}}{\epsilon_{436}^{NO_2}} \quad (5)$$

and so, from slope and intercept of a plot of A_{220}/A_{436} against A_{436} the two absorption coefficients can be determined. The results are shown in Figure 3. At 220 nm, with a bandwidth of 0.2 nm, the absorption coefficients for both NO_2 and N_2O_4 were found to increase by ≃40% from 1 to 200 bar of N_2.

(20) Chao, J.; Wilhoit, R. C.; Zwolinski, B. J. *Thermochim. Acta* **1974**, 359.

(21) Hsu, D. K.; Monts, D. L.; Zare, R. N. *Spectral Atlas of Nitrogen Dioxide 5580 to 6480 Å*; Academic: New York, 1978.

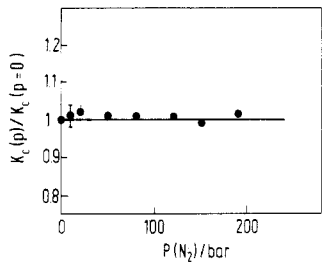

Figure 4. Dependence of the equilibrium constant $K_c = [NO_2]^2/[N_2O_4]$ on the N_2 bath gas pressure.

The quantitative dependence of K_c on the pressure of added bath gas is difficult to predict as the relevant molecular parameters are not known sufficiently. Decreases of K_c by factors of 2.5 and 4.4 for solutions in liquid heptane and CO_2, both at 65 bar pressure, have been reported.[22] The densities in both of these cases are respectively somewhat below and above that of, e.g., 200 bar of N_2 (7.6×10^{-3} mol cm^{-3}). A much smaller decrease of K_c by a factor 1.36 for a 1 to 200 bar increase of N_2 pressure is predicted on the basis of calculated fugacity coefficients. They were derived by a third-order virial expansion, which used standard averaging rules for the estimation of the unknown mixed second and third virial coefficients from data of the pure components.[23] Finally one may compare with the thermodynamic reaction volume ΔV_R ($= -RT\, d \ln K_p/dP$) of the N_2O_4 dissociation as it has been calculated from gas-phase electron diffraction data of the molecular geometries.[24] The value of ΔV_R has been estimated as 2.1 cm^3 mol^{-1} which implies that $K_p(200\text{ bar})/K_p(1\text{ bar}) = 0.98$. The experimental dependence of K_c on nitrogen pressure, as it follows from eq 4, is shown in Figure 4. Within the experimental error there is no change in K_c when the pressure of added N_2 is increased from 1 to 200 bar. This result indicates either very weak interaction forces between nitrogen and both the nitrogen oxides or some accidental compensation of effects. One may thus presume that the kinetics of association of NO_2 is not markedly influenced by effects from intermediate complex formation within the pressure range of this work. Such an effect has been observed, however, in the recombination of methyl radicals to form ethane,[25] where a non-diffusion-limited decrease of the high-pressure rate constant occurred above 50 bar of N_2, apparently due to chemical interaction with the bath gas.

The Rate of the Reaction $2NO_2 \rightarrow N_2O_4$. The primary photolysis of N_2O_4 at 248.4 nm (482 kJ mol^{-1}) can in principle proceed through three channels:

$$N_2O_4 + h\nu \rightarrow NO_2 + NO_2 \quad (6)$$

$$\rightarrow N_2O_3 + O \quad (7)$$

$$\rightarrow NO_3 + NO \quad (8)$$

The respective dissociation energies are 53, 310, and 148 kJ mol^{-1}. Also further dissociation of the N_2O_3 fragment is possible

$$N_2O_3 \rightarrow NO_2 + NO \quad (9)$$

which has a total energy requirement of 354 kJ mol^{-1}. However, previous quantum yield measurements[26] of electronically excited NO_2* produced in reaction 6 and recent molecular beam experiments with mass spectrometric and translational energy analysis[17] have shown that practically all of the N_2O_4, excited at 248 nm, decomposes via reaction 6 into NO_2 fragments excited into the $\tilde{A}$ or $\tilde{B}$ states.

TABLE I: Summary of the Measured Rate Coefficients, k_1, of the Reaction $NO_2 + NO_2 + N_2 \rightarrow N_2O_4 + N_2$ at 298 K[a]

$p(N_2)$/ bar	k_1/ 10^{14} cm^3 molecule^{-1} s^{-1}	$p(N_2)$/ bar	k_1/ 10^{14} cm^3 molecule^{-1} s^{-1}
0.91	2.57	12	15.0
2	4.26	20	20.9
3	6.46	50	32.2
4	8.05	80	38.2
5	8.58	120	45.3
6	9.95	160	46.2
8	11.6	203	51.8
10	15.1	207	51.3

[a] 20 Torr of NO_2/N_2O_4 mixture.

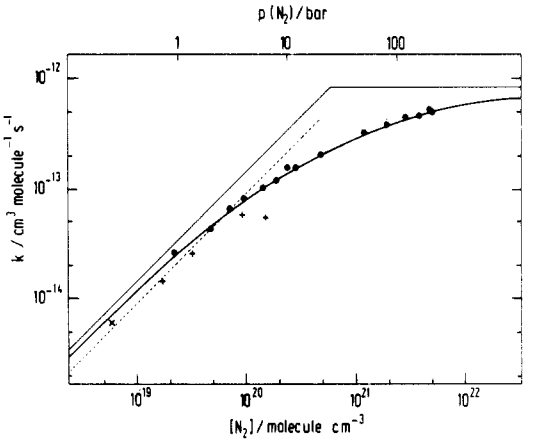

Figure 5. Falloff curve for the association reaction $NO_2 + NO_2$ ($+N_2$) $\rightarrow N_2O_4$ ($+N_2$) at 300 K. ×, ref 6; +, ref 7; ●, this work; broken line, k_1^0 recommended in ref 11; full line, this work; for details see text.

At the pressures in our experiments the electronically excited NO_2 states are rapidly quenched ($\tau = 10^{-9}$ s at 1 bar pressure[26]) and the rovibrational and translational energy will rapidly be dissipated, so that energy relaxation and the consequent temperature rise will be much faster than the association reaction. It has already been mentioned that 6% of the absorbed light at 248 nm excite NO_2 molecules. The consequent change of $\leq 5 \times 10^{-4}$ in the NO_2 concentration is negligible and of no importance for the mass balance of the N_2O_4/NO_2 system. The photolysis of NO_2 is known up to very high pressures[27,28] giving rise to a number of photoproducts. Detailed calculations, however, showed that formation and secondary reactions of such products like NO, NO_3, N_2O_3, and N_2O_5 do not interfere with the observations under our conditions. Some of the processes involving these nitrogen oxides proceed on the time scale of our measurement, but low concentrations and small absorption cross section prevent their detection at 220 nm. At room temperature and the very low amount of NO in our system even N_2O_3 reactions can only contribute with <0.3% to the observed changes of absorption at 220 nm although in this case $\epsilon(N_2O_3)$ is about 3.5 times larger than $\epsilon(N_2O_4)$.[29] In total we estimate less than 1% contribution to our signal from side reactions. Thus the experimental rate coefficient derived from the absorption at 220 nm is directly identified with the relaxation coefficient k_r in eq 3.

Table I gives our measured rate constants, k_1, for the $NO_2 + NO_2$ association reaction for pressures of added N_2 between 1 and 207 bar. Each value is the average of 4–20 measurements. The second-order rate constant increases with pressure but the pressure dependence of k_1 decreases markedly toward higher pressures. Figure 5 shows that the measurements cover the whole central part of the falloff regime and allow a reliable extrapolation to the high- and low-pressure rate constants, k_1^∞ and k_1^0. The corre-

(22) Wendelken, H.-J. Diploma Thesis, Göttingen, 1980.
(23) Reid, R. C.; Prausnitz, I. M.; Sherwood, Th. K. *The Properties of Gases and Liquids. Their Estimation and Correlation*; McGraw Hill: New York, 1980.
(24) Ewald, A. H. *Discuss. Faraday Soc.* **1956**, *22*, 138.
(25) Hippler, H.; Luther, K.; Ravishankara, A. R.; Troe, J. *Z. Phys. Chem. NF* **1984**, *142*, 1.
(26) Inoue, G.; Nakata, Y.; Usui, Y.; Akimoto, H.; Okuda, M. *J. Chem. Phys.* **1979**, *70*, 3689.
(27) Gaedtke, H.; Hippler, H.; Troe, J. *Chem. Phys. Lett.* **1972**, *17*, 174. Gaedtke, H.; Troe, J. *Ber. Bunsen-Ges. Phys. Chem.* **1975**, *79*, 184.
(28) Baulch, D. L.; Cox, R. A.; Hampson, R. F.; Kerr, J. A.; Troe, J.; Watson, R. T. *J. Phys. Chem. Ref. Data* **1980**, *2*, 295.
(29) Shaw, A. W.; Vosper, A. J. *J. Chem. Soc., Dalton Trans.* **1972**, 961.

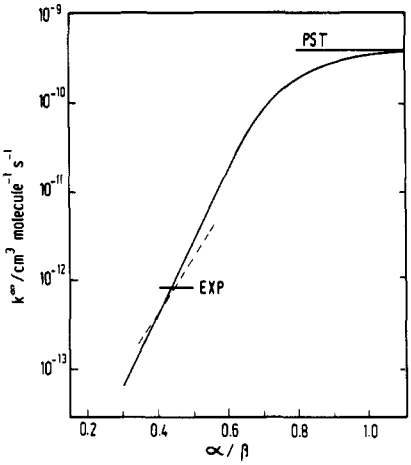

Figure 6. High-pressure association rate constants k_1^∞ for $NO_2 + NO_2 \rightarrow N_2O_4$ calculated by using the simplified statistical adiabatic channel model (SACM). k_1^∞ is shown as a function of the SACM parameter α/β. Microcanonical[17] (solid line) and canonical[31] (broken line) calculations. The phase space theory (PST) value and the experimental result of this work (EXP) are indicated.

sponding analysis was done by an iterative fitting of reduced falloff curves as described in the following sections. The limiting rate constants finally obtained are

$$k_1^0 = (1.4 \pm 0.2) \times 10^{-33}[N_2] \text{ cm}^3 \text{ molecule}^{-1} \text{ s}^{-1}$$

$$k_1^\infty = (8.3 \pm 1.0) \times 10^{-13} \text{ cm}^3 \text{ molecule}^{-1} \text{ s}^{-1}$$

Theoretical Analysis. Thermal High-Pressure Rate Constant, k^∞, and Specific Rate Constants, $k(E,J)$. The construction of a realistic falloff curve requires an analysis of k^∞. At first k^∞ is estimated empirically by an extrapolation of the experimental results. The theoretical analysis of this k^∞ then provides the parameters for a falloff curve which finally leads to an improved value of k^∞. An analysis of the low-pressure rate constant k^0 allows us to include weak collision effects of the falloff curve.

The statistical adiabatic channel model (SACM)[30] is well suited to the analysis of the high-pressure rate constants of association/dissociation reactions. It includes angular momentum effects which are known to have their greatest effects in bond fission reactions. Also, the model can be formulated with one free parameter only. This parameter may be fitted by one measurement and the model is then particularly useful for predictions of other observables. Here we fit the parameter from k^∞ and predict specific rate constants $k(E,J)$ with the simplified SACM version of ref 17, which has been previously tested in detail.

The microcanonical simplified SACM calculations[17] were run on an IBM PC-AT computer which produced a complete set of results within a few minutes. For a given value of α, the SACM looseness parameter of the N_2O_4 potential energy surface, values of $k(E,J)$ were calculated for a range of energy and J values. The thermal high-pressure rate constant was obtained by averaging of $k(E,J)$ over the thermal population distributions. Figure 6 shows the dependence of the calculated k^∞ on the ratio α/β, where β (=1.16 Å^{-1}) is the Morse parameter for the N–N reaction coordinate. The intersection of the calculated line with the experimental value of k^∞ allows one to fit $\alpha/\beta = 0.44$. Although the corresponding value of $\alpha = 0.51$ Å^{-1} is much smaller than that found in previous calculations for other reactions, the essential quantity in SACM calculations, i.e., the ratio α/β, is in close agreement with the "standard" value $\alpha/\beta = 0.46 \pm 0.09$, found for a wide range of other association/dissociation reactions.[32] The diagram also indicates k^∞ obtained from calculations done in the limit of phase space theory (PST), which corresponds to the case

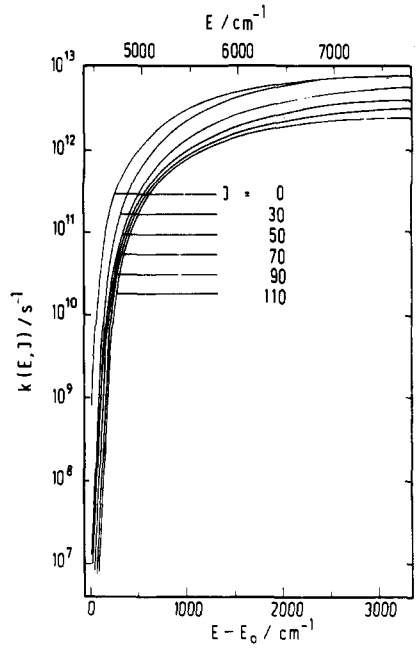

Figure 7. Specific rate constants $k_{-1}(E,J)$ for the dissociation of N_2O_4 at various values of J. Simplified SACM calculations; $\alpha/\beta = 0.44$.

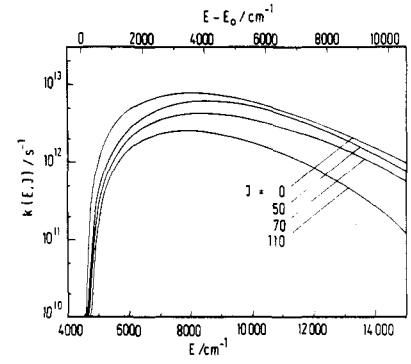

Figure 8. Specific rate constants $k_{-1}(E,J)$ for the dissociation of N_2O_4. Calculations as in Figure 7. The display over a wider energy range shows the occurrence of maxima at $\alpha/\beta = 0.44$ for various J.

of a completely "loose" transition state in SACM ($\alpha/\beta > 1$). The PST limit, calculated at $\alpha/\beta \gg 1$, is nearly 3 orders of magnitude greater than the experimental value.

k^∞ was also calculated separately with the canonical version of simplified SACM[31] and a plot of the results is included in Figure 6. The functional dependence on α/β differs a little from the microcanonical results because of the slightly differing coupling relations in the two treatments. Coupling between various coordinates is expressed by effective Morse parameters, $\beta_{eff}(E,J)$, and the present reaction turned out to be more sensitive to the choice of β_{eff} than other cases[33] (see also Appendix A). However, at the experimental value of k^∞ the agreement between the two methods of calculations is very good. At $\alpha/\beta = 0.44$ both calculations differ by less than 10% and the optimum choice of α/β for the canonical calculations is 0.45.

At a temperature of 600 K a value of 3.9×10^{-13} cm^3 molecule^{-1} s^{-1} was calculated for k_1^∞ by using $\alpha/\beta = 0.44$. A combined representation can be given for the temperature range 300 K $\leq T \leq$ 600 K:

$$k_1^\infty = 8.3 \times 10^{-13}(T/300 \text{ K})^{-1.1} \text{ cm}^3 \text{ molecule}^{-1} \text{ s}^{-1}$$

The corresponding expression for the N_2O_4 dissociation in the same temperature range is

$$k_{-1}^\infty = 7.7 \times 10^{15}(T/300 \text{ K})^{-1.1} \exp(-6460 \text{ K}/T) \text{ s}^{-1}$$

(30) Quack, M.; Troe, J. *Ber. Bunsen-Ges. Phys. Chem.* **1974**, *78*, 240.
(31) Troe, J. *J. Chem. Phys.* **1981**, *75*, 226. Cobos, C. J.; Troe, J. *J. Chem. Phys.* **1985**, *83*, 1010.
(32) Brouwer, L. D.; Müller-Markgraf, W.; Troe, J. *J. Phys. Chem.*, submitted for publication.
(33) E.g. Troe, J. *J. Phys. Chem.* **1984**, *88*, 4375. Cobos, C. J.; Hippler, H.; Troe, J. *J. Phys. Chem.* **1985**, *89*, 342.

Representative calculations of $k(E,J)$ for the dissociation of N_2O_4 are shown in Figure 7. While the qualitative pattern of the curves resembles that of other bond fission reactions, there are some pronounced differences. The increase of $k(E,J)$ above the threshold energy E_0 is exceedingly steep, showing a $>10^4$-fold increase within 3 kJ mol^{-1} (250 cm^{-1}). As a result of small rotational constants, the curves for various J are closely bunched together but they are not simply displaced along the energy scale. Crossing of curves with different J values, a pronounced feature in many bond fission reactions,[14,34,35] occurs only faintly for low J values. Furthermore the $k(E,J)$ curves display maxima. This is indicated more clearly in Figure 8, where a magnified scale for $k(E,J)$ and a larger range of energy are chosen. The figure shows $k(E,J)$ curves for $\alpha/\beta = 0.44$; in all cases maxima appear only about 3500 cm^{-1} above the reaction threshold. Such maxima in $k(E,J)$ curves have not been observed before in a range of energy and rate constant which is, in principle, accessible to experiments. We have therefore explored the conditions for such a behavior in more detail. This will be discussed in a following section.

Falloff Curve and Low-Pressure Rate Constant k^0. Expressions for the reduced falloff curve from ref 36 were used to represent the transition of k_1 between k_1^0 and k_1^∞:

$$\frac{k_1}{k_1^\infty} = \frac{k_1^0/k_1^\infty}{1 + k_1^0/k_1^\infty} F^{SC}(k_1^0/k_1^\infty) F^{WC}(k_1^0/k_1^\infty) \quad (10)$$

The broadening factors for strong and weak collisons, F^{SC} and F^{WC}, can be expressed by an approximate common relationship, which is well suited to room temperature applications

$$\log F^{SC}F^{WC} \simeq [1 + (N^{-1} \log (k_1^0/k_1^\infty))^2]^{-1} \log F_{cent} \quad (11)$$

The parameters F_{cent} ($=F^{SC}_{cent}F^{WC}_{cent}$) and N, which define the shape of the falloff curve, were evaluated with the expressions in ref 36 on the basis of the empirically derived values of k_1^∞ and k_1^0. This first falloff curve led to improved limiting rate constants which were used to obtain the parameters of the final falloff curve. The results are

$$F^{SC}_{cent} = 0.43; \quad F^{WC}_{cent} = 0.92; \quad N = 1.26$$

The low-pressure limiting rate constant for the dissociation, k_{-1}^0, was analyzed by using the factorized analytical expression of ref 37. The rotational factor, $F_{rot} = 5.74$ at 300 K, was determined for a Morse type interaction potential. Using the equilibrium constant K_c of ref 20, we found the strong collision rate coefficients to be $k_{1,SC}^0 = 2.6 \times 10^{-33}[N_2]$ and $5.1 \times 10^{-33}[N_2]$ cm^3 molecule^{-1} s^{-1} at $T = 300$ and 500 K, respectively. Comparison of $k_{1,SC}^0$ with k_1^0, obtained from the falloff analysis of the experimental results, gives a collision efficiency $\beta_c(N_2)$ of 0.54. Using the relation $\beta_c/(1 + \beta_c^{1/2}) = -\langle\Delta E\rangle/F_E kT$,[38] we derived a value of -560 cm^{-1} for $\langle\Delta E\rangle$, the average energy transferred per collision. This value of $-\langle\Delta E\rangle$ appears high for collisions with N_2; but the error limits are inherently wide in this type of derivation of $\langle\Delta E\rangle$, as uncertainties in the calculation of k_{SC}^0 are projected on the β_c values with increased weight. Small changes of β_c are, however, sufficient to arrive at normal, lower values for $\langle\Delta E\rangle$ of N_2. With the assumption that $\langle\Delta E\rangle(N_2)$ is independent of temperature up to 500 K, $\beta_c(N_2,500\text{ K})$ follows as 0.42 and the temperature dependence of k_1^0 is given by

$$k_1^0 = 1.40 \times 10^{-33}(T/300\text{ K})^{-3.8}[N_2] \text{ cm}^3 \text{ molecule}^{-1} \text{ s}^{-1}$$

for temperatures between 300 and 500 K. For the dissociation in the same temperature range one has

$$k_{-1}^0 = 1.29 \times 10^{-5}(T/300\text{ K})^{-3.8} \exp(-6460\text{ K}/T)[N_2] \text{ s}^{-1}$$

Discussion

Comparison with Previous Measurements. Figure 5 includes results from earlier work using N_2 as a bath gas. The agreement is good particularly considering the difficulties in the early experiments. Carrington and Davidson[7] were the only ones who used pressures considerably above 1 bar. Up to 7 bar of N_2 and similarly in CO_2 they observed deviations from third-order behavior (in terms of the association reaction). From their data at the lower pressures as well as from others below 1 bar in pure NO_2/N_2O_4 or with added Ar or He,[5,6] it was concluded that reactions 1,−1 were at their low-pressure limit below 1 bar pressure. Correspondingly, data evaluations give k_1^0 to be $8.2 \times 10^{-34}[N_2]$ cm^3 molecule^{-1} s^{-1} [11] (average from ref 6 and 7) or $6.6 \times 10^{-34}[N_2]$ cm^3 molecule^{-1} s^{-1} [12] (from ref 7). However, our results from Figure 5 show that there are still deviations from third-order behavior at pressures below 1 bar, and consequently k_1^0 is larger than the measured rate constants. Figure 5 also shows that the falloff curve has to be measured over a large pressure range in order to reveal the curvature close to the low-pressure limit. The present work has fulfilled this condition. Using the reduced falloff expression with its given curvature, the fitting to the experimental points is most sensitive in the center of the falloff range. Therefore, our high-pressure data from that range contribute very strongly to the quantitative determination of the k_1^0 value.

Recent relaxation studies on the NO_2 association, using temperature jumps induced by absorption of pulsed CO_2 laser radiation,[10,13] also show deviations from third-order behavior. These data from measurements at lower temperatures appear to agree well with the present results. However, a ratio of the apparent third-body efficiency of N_2O_4/NO_2 to Ar of 40 is reported at 260 K which, if confirmed at 300 K, would lower our rate coefficients in N_2 at the lowest pressures. But a high third-body efficiency of N_2O_4/NO_2 should then also appear in the reverse reaction. Dissociation studies of N_2O_4 have so far only recorded relative efficiencies between N_2O_4/NO_2 and N_2 of ~ 2.[11] Also data from a recent study of $NO + NO_2 \rightarrow N_2O_3$,[39] a system similar to N_2O_4, do not indicate an exceptional effect of NO_2/NO as a third body even at temperatures as low as 210 K.

k_∞ and $k(E,J)$. Apart from very approximate estimates, based on oversimplified models,[7] or questionable extrapolations from data at pressures close to 1 bar,[5b] the limiting high-pressure rate constants k_1^∞ or k_{-1}^∞ have not been published.[13] The value of k^∞ for the association step in the weakly bound N_2O_4/NO_2 system is much lower than those for most other radical association reactions.[32] An analysis of this apparently unusual kinetic parameter, k^∞, and of the corresponding specific rate constants, $k(E,J)$, may thus show characteristic features which appear far less pronounced in the strongly bound, "normal" bond fission/association systems. The noticeable low value of k^∞ from this work, until now surpassed only by k^∞ of the large molecule $F_2S_2O_6$,[40] can be well understood in terms of a SACM analysis. Factorization of k^∞ into the rate constant k^∞_{loose} from phase space theory and into a "rigidity" factor f^∞_{rigid} ($=k^\infty/k^\infty_{loose}$) shows that only the extremely small $f_1^\infty{}_{rigid}$ of 2×10^{-3} causes the low value of k^∞, while $k_1^\infty{}_{loose} = 4.1 \times 10^{-10}$ cm^3 molecule^{-1} s^{-1} is in the normal range of many systems analyzed previously.[32] The origin of this small "rigidity" factor lies in the low frequencies of oscillators disappearing in the N_2O_4 dissociation and small rotational constants of the correlated product rotations. The still lower f^∞_{rigid} recently found in the reaction system $FSO_3 + FSO_3 \rightleftarrows F_2S_2O_6$[40] follows the same trends due to its even smaller rotational constants.

One might be inclined to interpret the large difference between k^∞ and the PST limit, k^∞_{loose}, or the small α-value of $\alpha = 0.51$ as indications of an unusually tight transition state. However, it is the ratio α/β which determines the character of the reaction

(34) Brouwer, L.; Cobos, C. J.; Troe, J.; Dübal, H.-R.; Crim, F. F. *J. Chem. Phys.* **1987**, *86*, 6171.
(35) Luther, K.; Troe, J. *Proceedings of the 17th Symposium on Combustion*; Combustion Institute; Pittsburgh, PA, 1979; p 535.
(36) Troe, J. *J. Phys. Chem.* **1979**, *83*, 114. Gilbert, R. G.; Luther, K.; Troe, J. *Ber. Bunsen-Ges. Phys. Chem.* **1983**, *87*, 169. Luther, K.; Troe, J. In *Reactions of Small Transient Species*; Fontijn, A., Clyne, M. A. A., Eds.; Academic: London, 1983; p 63.
(37) Troe, J. *J. Chem. Phys.* **1977**, *66*, 4758.
(38) Troe, J. *J. Chem. Phys.* **1977**, *66*, 4745.
(39) Smith, I. W. M.; Yarwood, G. *Chem. Phys. Lett.* **1986**, *130*, 24; *Faraday Discuss. Chem. Soc.* **1987**, *84*, paper 11.
(40) Cobos, C. J.; Croce de Cobos, A. E.; Hippler, H.; Castellano, E. *J. Phys. Chem.*, submitted for publication.

potential varying between $\alpha/\beta \simeq 0$ for "tight" and $\alpha/\beta \gg 1$ for "loose" situations. The value $\alpha/\beta = 0.44$ for the N_2O_4 system agrees well with the "standard" ratio $\alpha/\beta = 0.46 \pm 0.09$ from previous applications of SACM.[32] Therefore the present system behaves completely normal; i.e., the relative character of the N_2O_4 reaction potential with respect to its radial and angular components is of a typical intermediate character. The association of two OH forming H_2O_2 is a nicely contrasting example which is normal as well, having the same $\alpha/\beta = 0.44$ ($\alpha = 1.08$ Å^{-1}) as N_2O_4 but with the rigidity factor f^{∞}_{rigid} as high as 0.45. The low α value of N_2O_4 simply goes together with a small Morse parameter of the N–N bond, $\beta = 1.16$ Å^{-1}. N_2O_4 is thus a good example for the surprising universality of a standard value of the ratio α/β in bond fission reactions, while the choice of a fixed value for α appears less appropriate.

Further insight into the peculiarities of the N_2O_4/NO_2 system can be gained by considering the $k(E,J)$ curves for N_2O_4 dissociation shown in Figures 7 and 8 for the lower and higher energy ranges. The two striking features are the extremely steep rise of $k(E,J)$ over several orders of magnitude, just above threshold energy, and the maxima in each of the curves. These are closely related phenomena having their origin in the combined effects of several disappearing low-frequency oscillators, and the small bond dissociation energy of a large molecule.

The functional dependence of $k(E,J)$ on E is determined by the interplay between the energy dependencies of the number of open reaction channels $W(E,J)$ and the density of the reactant states $\rho(E,J)$:

$$k(E,J) = W(E,J)/h\rho(E,J) \qquad (12)$$

A very rapid increase of $W(E,J)$ is responsible for the steep rise of $k(E,J)$ at low energies. The energy dependence of $\rho(E,J)$ is, of course, weaker but it does not contribute to the rise of $k(E,J)$ through a particularly slow increase with energy. In N_2O_4 the effects of several disappearing oscillators accumulate, each of which transforms into a product rotor with a small rotational constant. In such cases there is also a marked dependence of $k(E,J)$ on the α/β parameter observed and the initial rise of $k(E,J)$ becomes even more accentuated at larger α/β values as the case of a loose transition complex is approached.

The pronounced contribution of several disappearing oscillators is also responsible for the maxima in the $k(E,J)$ curves. The rotorlike character of the disappearing oscillators at high energies gives rise to a weaker energy dependence $dW(E,J)/dE$ than would be obtained with pure oscillators. One may rationalize the effect by considering classical degrees of freedom. For an activated complex of s harmonic oscillators, one would have $W(E) \propto (E - E_0)^s$. If $l = 6$ disappearing oscillators reach rotorlike energy dependence ($\propto E^{0.5}$) this leads to $W(E) \propto (E - E_0)^{s-6+3}$. Assuming the usual $\rho \propto E^{s-1}$, the energy dependence of $W(E)/\rho(E) \propto (E - E_0)^{s-3}/E^{s-1}$ and may approach a dependence $\propto E^{-2}$ at sufficiently high energies. Maxima in $k(E,J)$, in principle, can thus occur even for this simple model. In N_2O_4 very flat maxima of essentially this type became visible at rather high energies ($\gtrsim$15 000 cm) in model calculations for uncoupled oscillators at $J = 0$. Figure 9b shows part of such curves $k_\beta(E,J=0)$, calculated with constant $\beta_{eff} = \beta$ (see also further down).

Complete SACM calculations showed, however, more pronounced maxima at lower energies (Figures 8 and 9a). The most important of several contributions to the shapes and positions of the maxima come from coupling between the various disappearing oscillators of the reactant. The effective potential of a disappearing oscillator changes due to the energy located in other disappearing modes. In the simplified SACM this is taken into account by modification of the reactant Morse parameter β into $\beta_{eff}(E)$, an increasing function of energy. (For the calculation of β_{eff} see also Appendix A). Figure 9 demonstrates for N_2O_4 in $J = 0$, how the additional rigidity from mode coupling affects the energy dependence of $W(E,J)$ and therefore the shape of the $k(E,J)$ curves. The $k(E,J=0)$ curves in Figure 9, a, b, and c, for α/β of 0.3, 0.44, and 1.03, respectively, can be factorized according to $k(E,J=0) = k_\beta(E,J=0)$. $\gamma_c(E)$ and these both factors are shown in Figure

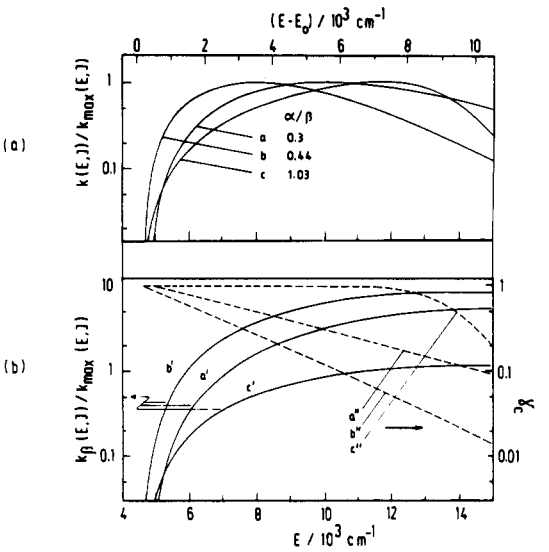

Figure 9. Influence of coupling of "disappearing" modes on the maxima in $k(E,J)$ curves at $\alpha/\beta = 0.3$ (a,a',a''), 0.44 (b,b',b''), and 1.03 (c,c',c''). $k(E,J) = k_\beta(E,J)$. $\gamma_c(E,J)$ is considered in the case of $J = 0$. (a) Specific rate constants $k(E,J=0)$ for N_2O_4 dissociation. Each curve is normalized to its maximum $k_{max}(E,J)$. (b) Specific rate constants $k_\beta(E,J=0)$ for uncoupled modes (SACM, constant $\beta_{eff} = \beta$), full lines (a',b',c'). Ratio, $\gamma_c = W(\beta_{eff})/W(\beta)$, of open reaction channels with and without mode coupling (introduced in SACM through the use of $\beta_{eff}(E,J)$), broken lines (a'',b''c'').

9b as curves a', b', c', and a'', b'', c'', respectively. Here k_β is the rate constant for the case of uncoupled modes (calculated by using a constant $\beta_{eff} = \beta$) and γ_c is the ratio between the numbers of open reaction channels with and without contribution from the coupling of disappearing modes, $W(\beta_{eff})/W(\beta)$. The dependence of γ_c on energy, introduced via the increase of $\beta_{eff}(E)$ varies considerably with the value of α/β ($=\alpha/\beta_{eff}(E_0)$). γ_c decreases faster and the maximum of $k(E)$ is shifted further to lower energies at $\alpha/\beta = 0.44$ (curves b'' and b) than at $\alpha/\beta = 0.3$ (curves a'' and a). In the case of a loose transition complex, $\alpha/\beta = 1.03$, the decrease in γ_c (curve c'') and the occurrence of a maximum in $k(E)$ (curve c) are shifted to high energies beyond 6000 cm^{-1} above threshold. These variations of γ_c with α/β and the corresponding shifts in the position of the $k(E,J)$ maxima are easily rationalized, considering the functional dependence of W (or of k_β) on α/β. Initially this dependence increases a α/β grows; but it levels off at higher α/β values and reaches the phase space limit. (For a similar type of functional dependence on α/β, see Figure 6.) The consequences of some relative decrease are therefore most pronounced whenever the effective α/β is in a range of intermediate values. In the loose complex situation, with $\alpha/\beta \simeq 1$ at E_0, a considerable decrease in α/β has to occur until, at higher energies, $\gamma_c \ll 1$ will result.

Rotational excitation of the reactant, $J > 0$, affects W through angular momentum constraints and enhances the rigidity of the effective potentials. A decrease in the maximum value of $k(E,J)$ for N_2O_4 with increasing J is therefore expected and observed as some examples in Figure 8 show.

The general results of the present work on the occurrence of maxima in $k(E,J)$ of N_2O_4 bond fission can be summarized in three points: (i) Maxima of $k(E,J)$ have been found for a wide variety of potential parameters ($0.3 \leq \alpha/\beta \leq 4$) including rather tight as well as completely loose cases (PST limit). (ii) Maxima were found for widely varying cases of coupling relationships, from total neglect of coupling to clear overcorrection. (iii) The qualitative tendencies of positions and shapes of maxima follow the expectations based on simple models, see above.

The predicted maxima in $k(E,J)$ of N_2O_4 are at sufficiently low values, reaching down to about 10^{12} s^{-1}, such that they are, in principle, accessible to direct experiments. The positions of the maxima at very low excess energies and their pronounced shapes are other favorable features for an empirical verification of this type of energy dependence of $k(E,J)$ in either N_2O_4 or a

system with similar parameters.

In conclusion, the NO_2/N_2O_4 system represents a model for association/dissociation reactions with small threshold energy. As a consequence low high-pressure rate constants and very steep $k(E,J)$ curves with maxima at low energies are obtained. The SACM provides a convenient and realistic approach for a theoretical rationalization of these effects.

Acknowledgment. We thank Professor J. Troe for stimulation and helpful discussions, Dr. H. Hippler for his involvement in the experiments, and Dr. L. Brouwer for the preparation of programs and some calculations. P.B. thanks the Royal Society of London and the Deutsche Akademische Austauschdienst for grants. This work was supported by the Deutsche Forschungsgemeinschaft within the Sonderforschungsbereich 93 "Photochemie mit Lasern".

Appendix A

Effective Morse Parameters of Reaction Channel Potentials. In simplified SACM calculations the energy pattern is considered separately[17,31] of each oscillator which disappears together with that in the reaction coordinate. The amounts of energy in all other molecular modes influence the effective channel potential for the oscillator just under consideration. To take this into account the Morse parameter β and D of the reaction channel potential are modified into β_{eff} and D_{eff}, all related by $\beta_{eff}(E,J) = \beta[D/D_{eff}(E,J)]^{0.5}$. $D_{eff} = D' + E_c$ includes a rotational energy correction in $D' = D + E_0(J) - E_0 - B_eJ(J+1)$.[17,35] The remaining term, E_c, represents a superposition of energy terms from the other (mainly from the likewise disappearing) modes and can be applied to very different degrees of approximation. We have tried various expressions for E_c, using eq 2,13 of ref 17 (I), the more general result of ref 35, eq A1-A3 (II), and an alternative expression developed along the same lines of reasoning as the previous

$$D_{eff} = D' + (E - E_0)(b-1)/b + (s-2)M/2(s-1)N\{[1 + 4N(E-E_0)(b-1)/bM^2]^{0.5} - 1\} \quad \text{(III)}$$

The nomenclature used here is that of ref 35, Appendix A. The $k(E,J)$ results given above were calculated with D_{eff}(III). The first alternative (I), shown to be quite sufficient in several cases,[33] deviates by about a factor 10 over much of the $k(E,J)$ curves and in k_∞ from calculations with the latter two more detailed corrections, which differ only somewhat at high energies but agree within 10% on the thermal averaged k_∞. However, it was found that the results on the basis of eq III, which treats individually the contributions from all modes, could also be well reproduced for all $k(E,J)$ by using the simple expression

$$D_{eff} = D' - (b-1)[E - E_0 - B_EJ(J+1)]/s \quad \text{(IV)}$$

Appendix B

Molecular Parameters for Modelling N_2O_4 Bond Fission. N_2O_4 frequencies (in cm^{-1}): 1368, 812, 266, 79, 1709, 475, 422, 659, 1742, 375, 1251, 743, from ref 41 and 42. Barrier for internal rotation: 875 cm^{-1}.[43] NO_2 frequencies (in cm^{-1}): 1665.5, 1357.8, 756.8.[44] Rotational constants (in cm^{-1}): N_2O_4, 0.2713, 0.1174, 0.0804 (calculated from the geometry of ref 45); NO_2, 8.0012, 0.4336, 0.4104.[44] Threshold energy ΔH_0^0 = 53.2 kJ mol^{-1}.[44] Reaction coordinate: 266 cm^{-1}. Force constant for the N-N bond: 0.3 mdyn $Å^{-1}$.[41] Correlations of transitional modes (in cm^{-1}): 375 ↔ 0.4336, 659 ↔ 8.0012, 475 ↔ 8.0012, 422 ↔ 0.4336, 79 ↔ 0.4104, 0.2173 ↔ 0.4104. Lennard-Jones parameters: N_2O_4, σ = 4.62 Å, ϵ/k = 347 K; NO_2, σ = 3.77 Å, ϵ/k = 210 K; N_2, σ = 3.74 Å, ϵ/k = 82 K.

Registry No. NO_2, 10102-44-0; N_2O_4, 10544-72-6.

(41) Laane, J.; Ohlsen, J. R. *Prog. Inorg. Chem.* **1980**, *27*, 465.
(42) Holland, R. F.; Maier II, W. B. *J. Chem. Phys.* **1983**, *78*, 2928.
(43) Bibaut, C. H.; Ewing, G. E. *J. Chem. Phys.* **1974**, *61*, 1284.
(44) Stoll, D. R., Prophet, H., Eds. *JANAF Thermochemical Tables*; NSRDS-NBS 37, 2nd ed.; National Bureau of Standards: Washington, D. C., 1971.
(45) McClelland, B. W.; Gunderson, G.; Hedberg, K. *J. Chem. Phys.* **1972**, *56*, 4541.

Simulation of OH Radical Profiles in Premixed Atmospheric-Pressure Flat Flames

E. W. Kaiser

Chemistry Department, Research Staff, Ford Motor Company, Dearborn, Michigan 48121-2053
(Received: December 8, 1987)

OH profiles measured in the postflame gases of three propane–air (ϕ = 0.63, 1.17, 1.46) flames and one (ϕ = 1.01) methane–air flame at atmospheric pressure are compared with computer-simulated profiles generated by using a 15-reaction chemical mechanism. The simulated profiles deviate from the measured data by less than 15% for all four flames. Sensitivity analyses verify that reactions of the HO_2 radical determine the shape of the OH decay profile for the lean flame. For stoichiometric and rich flames, the radical recombination reaction (H + OH + M) strongly influences the OH radical profile. Experimental measurements of the CO, H_2, and O_2 profiles in lean and stoichiometric flames are also simulated correctly by the mechanism. For the stoichiometric flame, the experimental results verify that the H_2, O_2, and OH densities are in partial equilibrium in the postflame gases as predicted. These results provide a set of reaction rate constants and diffusion coefficients which correctly simulate the observed data over a wide range of fuel–air equivalence ratios.

Introduction

In order to test chemical kinetic mechanisms of combustion in flames, measured chemical species profiles must be compared to those generated by computer simulation. Available computer codes[1] allow the simulation of all of the major features which influence flame combustion, including convective flow, molecular and thermal diffusion, and detailed chemical kinetics. Recently, profiles of the hydroxyl radical in the postflame gas of laminar propane- or methane–air flames have been determined as a function of height at a variety of initial conditions above a flat-flame burner.[2] In this paper, the measured profiles are compared to those generated by computer simulation. The results provide a test of the chemical kinetics of selected reactions which occur in the H_2–O_2–CO–CO_2 reaction system at temperatures of 1600–1900 K.

(1) (a) Westbrook, C. K.; Dryer, F. L. *Prog. Energy Combust. Sci.* **1984**, *10*, 1. (b) Kee, R. J.; Grcar, J. F.; Smooke, M. D.; Miller, J. A. Sandia National Laboratories, Livermore, CA, Report SAND85-8240, 1985.

(2) Kaiser, E. W.; Marko, K.; Klick, D.; Rimai, L.; Wang, C. C.; Shirinzadeh, B.; Zhou, D. *Combust. Sci. Technol.* **1986**, *50*, 163.

0022-3654/88/2092-4384$01.50/0